

NJC

Accepted Manuscript



This is an *Accepted Manuscript*, which has been through the Royal Society of Chemistry peer review process and has been accepted for publication.

Accepted Manuscripts are published online shortly after acceptance, before technical editing, formatting and proof reading. Using this free service, authors can make their results available to the community, in citable form, before we publish the edited article. We will replace this *Accepted Manuscript* with the edited and formatted *Advance Article* as soon as it is available.

You can find more information about *Accepted Manuscripts* in the [Information for Authors](#).

Please note that technical editing may introduce minor changes to the text and/or graphics, which may alter content. The journal's standard [Terms & Conditions](#) and the [Ethical guidelines](#) still apply. In no event shall the Royal Society of Chemistry be held responsible for any errors or omissions in this *Accepted Manuscript* or any consequences arising from the use of any information it contains.

Cite this: DOI: 10.1039/c0xx00000x

www.rsc.org/xxxxxx

ARTICLE TYPE

Targeted doxorubicin delivery to hepatocarcinoma cells by lactobionic acid-modified laponite nanodisks†

Guangxiang Chen^{a,‡}, Du Li^{b,‡}, Jingchao Li^a, Xueyan Cao^a, Jianhua Wang^{*c}, Xiangyang Shi^{**a,b}, Rui Guo^{*a}*Received (in XXX, XXX) Xth XXXXXXXXX 20XX, Accepted Xth XXXXXXXXX 20XX*

DOI: 10.1039/b000000x

In this study, we covalently conjugated polyethylene glycol-linked lactobionic acid (PEG-LA) onto the surface of laponite (LAP) nanodisks for targeted delivery of doxorubicin (DOX) to liver cancer cells. LAP nanodisks were firstly modified with 3-aminopropyltrimethoxysilane to introduce amino groups on the surface, and then PEG-LA were successfully conjugated to form targeted LM-PEG-LA nanodisks via EDC chemistry. Finally, anticancer drug DOX was encapsulated into the synthesized nanocarriers with an exceptionally high loading efficiency of 91.5%. In vitro release studies showed that LM-PEG-LA/DOX could release drugs in a sustained manner with a higher speed at acid condition than at physiological one. MTT assay results proved that LM-PEG-LA/DOX displayed a significant higher therapeutic efficacy in inhibiting the growth of hepatocellular carcinoma cells (HepG2 cells) than 15 untargeted ones at the same DOX concentration. The targeting specificity of LM-PEG-LA/DOX was further demonstrated by flow cytometric analysis and confocal laser scanning microscopy. The developed LA-modified LAP nanodisks could serve as a targeted carrier for efficient loading and specific delivery of different anticancer drugs to liver cancer cells.

Introduction

Developing efficient drug delivery systems (DDS) has been a major challenge in cancer chemotherapy. Till now, various types of nano-devices, such as micelles,^{1, 2} dendrimers,^{3, 4} carbon nanotubes,^{5, 6} and nanoclays⁷ have been used to encapsulate anticancer drugs, and the obtained DDS display significant advantages in improving the solubility of drugs, controlling drug release properties, and passively targeting tumor tissues through EPR effect.⁸ However, those systems still inevitably cause undesirable side effects due to the lack of tumor-specific delivery. Therefore, specific peptides (RGD^{9, 10}) or biological ligands (folic acid,^{11, 12} hyaluronic acid,¹³ etc¹⁴⁻¹⁶) with an enhanced binding affinity toward certain receptors expressed by cancer cells have been attached onto the surface of nanocarriers to construct targeted drug delivery systems.

Asialoglycoprotein receptor (ASGPR) has been demonstrated to have high expression on the surface of hepatocytes and several human carcinoma cell lines, and show strong binding efficiency with galactose.¹⁷⁻²¹ Therefore, galactose-bearing lactobionic acid (LA) has been exploited as a targeting agent to realize targeted delivery to liver cancer cells. For example, Xu et al. used LA-conjugated dioleoylphosphatidyl ethanolamine as a component to build docetaxel-loaded solid lipid nanoparticles, and proved that this delivery system showed lower systemic toxicity and targeted antitumor efficacy in murine model.²² Villa et al. synthesized LA-modified chitosan microbubbles to deliver doxorubicin (DOX) to hepatocarcinoma cells specifically.¹⁶ In our previous studies, LA was linked on polyamidoamine dendrimer directly or through

poly(ethylene glycol) as a spacer, which endowed dendrimers the active targeting ability to hepatocarcinoma cells.^{15, 23} All these studies clearly demonstrated that attachment of LA could improve the specific accumulation of nanocarriers in tumors and increase the cellular uptake by cancer cells overexpressing ASGPR via receptor-mediated endocytosis.

In recent years, Laponite (LAP), a kind of synthetic clay, has attracted much attention in drug delivery applications due to its unique structure and properties.²⁴ It has a typical layered structure similar to natural hectorite, and can be stably dispersed in water with a diameter of about 25 nm and a thickness of 1 nm for each platelet. Hence, various of drug molecules, such as tetracycline,²⁵ amoxicillin,²⁶ and itraconazole,^{27, 28} can be inserted in the layered structure of LAP forming a sandwich-like drug delivery system. Among them, positively charged drug molecules could be encapsulated within LAP with extremely high payloads due to the negatively charged surface of LAP and its high cationic exchange capacity.^{29, 30} In our previous work, positively charged DOX molecules were encapsulated within LAP with a loading efficiency of 98.3%, and LAP/DOX showed a better therapeutic efficacy than free DOX in vitro.³¹ Following work demonstrated that LAP/DOX nanodisks passively targeted tumors via the enhanced permeability and retention (EPR) effect and displayed a better in vivo antitumor efficacy than free DOX.³² However, the lack of specificity to cancer cells is still an impassable barrier in the application of LAP-based drug delivery system. Therefore, it is highly desirable to modify LAP nanodisks with targeting functionalities in order to fully unleash the potential of LAP as a nanocarrier for drug delivery.

In this paper, we synthesized PEG-LA modified LAP nanodisks for targeted delivery of anticancer drug DOX to liver cancer cells. First, amine groups were introduced on LAP nanodisks through the surface modification of 3-aminopropyltrimethylethoxysilane (APMES). And then PEG-linked LA (LA-PEG-COOH) and PEG monomethyl ether with one carboxyl terminal group (*m*PEG-COOH) were covalently bonded on nanodisks via EDC chemistry to form targeted LM-PEG-LA and untargeted LM-*m*PEG carriers, respectively. And their structures and properties were extensively characterized by TGA, TEM, ¹H NMR, FTIR spectrometry, and dynamic light scattering (DLS). After loading DOX, the complexes were further evaluated by UV-vis spectroscopy and DLS. In vitro drug release was performed under both acidic and physiological conditions. Furthermore, in vitro antitumor efficacy of drug-loaded nanodisks was determined via MTT assay on a hepatocellular carcinoma cell line (HepG2 cell). Finally, the targeted delivery and intracellular uptake of LM-PEG-LA/DOX nanodisks were investigated by flow cytometry (FCM) and confocal laser scanning microscopy (CLSM).

Experimental

Materials

LAP was purchased from Zhejiang Institute of Geologic and Mineral Resources, and DOX•HCl was purchased Beijing Huafeng Pharmaceutical Co., Ltd.. Lactobionic acid (LA), 3-aminopropyltrimethylethoxysilane (APMES), 1-ethyl-3-[3-dimethylaminopropyl] carbodiimide hydrochloride (EDC), and N-hydroxysuccinimide (NHS) were from J&K Chemical Ltd.. PEG monomethyl ether with one end of carboxyl group (*m*PEG-COOH, Mw = 2000) and a dual functional PEG with one end of amine group and the other end of carboxyl group (NH₂-PEG-COOH, Mw = 2000) were from Shanghai Yanyi Biotechnology Corporation. All the other chemicals and solvents were purchased from Sinopharm Chemical Reagent Co., Ltd. (China). HepG2 cells (a human liver adenocarcinoma cell line) and MCF-7 cells (a human breast cancer cell line) were obtained from the Institute of Biochemistry and Cell Biology (the Chinese Academy of Sciences, Shanghai, China). Dulbecco's modified eagle medium (DMEM) medium, minimum essential medium (MEM) medium, fetal bovine serum (FBS), penicillin, and streptomycin were from Hangzhou Jinuo Biomedical Technology. MTT and Hoechst 33342 were from Sigma. All of the cell culture flasks and plates were from NEST Biotechnology (Shanghai, China). Water used in all experiments was purified using a Milli-Q Plus 185 water purification system (Millipore, Bedford, MA) with resistivity higher than 18 MΩ·cm.

Preparations

LM-NH₂ nanodisks. LAP was modified with APMES to introduce amino groups on the surface, as shown in Scheme 1. Briefly, LAP was dispersed in water at the concentration of 10 mg/mL under vigorous magnetic stirring overnight until a homogeneous solution was obtained. Then, an APMES solution was prepared by diluting 100 μL of APMES in 4.90 mL of water, and then was dropwise added into 25 mL of LAP solution. The reaction was undertaken at 50 °C water bath for 16 h. Finally, the reaction mixture was dialyzed against water (9 times, 2 L) for 3 d

using a dialysis membrane with a molecular weight cutoff of 8000-14000 to obtain the product LM-NH₂.

LA-PEG-COOH nanodisks. LA-PEG-COOH was synthesized according to our previous report.¹⁵ Briefly, LA (0.1 mmol, 35.83 mg), equal molar equivalents of EDC (19.17 mg) and NHS (11.50 mg) were dissolved in NaH₂PO₄-Na₂HPO₄ buffer (pH = 6.0, 0.02 M, 10 mL) under vigorous magnetic stirring for 3 h. Then, the activated LA solution was dropwise added to equal molar equivalent of NH₂-PEG-COOH solution and stirred for 3 d at room temperature. The reaction mixture was dialyzed against water (9 times, 2 L) using a dialysis membrane (MWCO of 500-1000) for 3 d to remove the excess reactants. Finally, the pure product LA-PEG-COOH was obtained by lyophilization.

LM-PEG-LA nanodisks. LA-PEG-COOH (34.27 mg, in 5 mL of water) was first activated by five molar equivalents of EDC and NHS with vigorous stirring for 3 h. The activated LA-PEG-COOH was dropwise added into the LM-NH₂ solution (6.276 mL, 52.33 mg) under vigorous shaking. After 3 days, the reaction mixture was dialyzed against water (9 times, 2 L) for 3 d using a dialysis membrane (MWCO of 8000-14000) to remove the excess reactants to get LM-PEG-LA. As a control, untargeted LM-*m*PEG was also synthesized by conjugating *m*PEG-COOH on LM-NH₂ by a similar method.

Characterization techniques

¹H NMR spectra were collected using a Bruker AV400 nuclear magnetic resonance spectrometer. Samples were dissolved in D₂O before measurements. FTIR spectrometry was performed using a Nicolet Nexus 670 FTIR (Nicolet-Thermo) spectrometer. All spectra were recorded using a transmission mode with a wavenumber range of 650-4000 cm⁻¹. TEM was performed using a JEOL 2010F analytical electron microscope (JEOL, Japan) operating at 200 kV. An aqueous solution of nanodisks (1 mg/mL) was dropped onto a carbon-coated copper grid and air dried before measurements. Thermogravimetric analysis (TGA) was carried out using a TG209F1 (NETZSCH Instruments Co., Ltd., Germany) thermogravimetric analyzer. The samples were heated from room temperature to 700 °C at a rate of 20 °C/min under nitrogen atmosphere. Zeta potential and dynamic light scattering (DLS) measurements were carried out using a Malvern Zetasizer Nano ZS model ZEN3600 (Worcestershire, U.K.) equipped with a standard 633 nm laser.

Loading of DOX

The concentrations of LM-PEG-LA and LM-*m*PEG solution were set at 6 mg/mL, and an aqueous solution of DOX (2 mg/mL) was prepared. Then, equal volume of DOX and carrier solutions were mixed and magnetically stirred for 24 h to ensure the sufficient interact and encapsulating. The mixture solutions were then centrifugated (5000 rpm, 10 min) and resuspended in water for 3 times to remove the unloaded free DOX. Finally, LM-PEG-LA/DOX and LM-*m*PEG/DOX solutions were stored in dark at room temperature. To determine the drug loading efficiency, the supernatants after 3 times centrifugation were collected, and the free DOX concentration in the supernatants was quantified using Lambda 25 UV-vis spectrophotometer (Perkin Elmer) at 480 nm with the standard absorbance-concentration calibration curve at the same wavelength. The drug

loading efficiency and drug loading content of DOX were calculated according to the following equations:

$$\text{Drug loading efficiency (\%)} = (W_0 - W_s) / W_0 \times 100\%$$

$$\text{Drug loading content (\%)} = (W_0 - W_s) / W_L \times 100\%$$

where W_0 , W_s and W_L represent the initial DOX mass, the DOX mass in the supernatant, and the mass of nanocarriers respectively.

Release of DOX from LM-PEG-LA/DOX

The in vitro release kinetics of DOX from LM-PEG-LA/DOX nanodisks under different pH conditions (pH = 5.4 and 7.4) were monitored using UV-vis spectroscopy. Briefly, 2 mL of LM-PEG-LA/DOX nanodisks (2.5 mg/mL) were placed in a dialysis bag with a MWCO of 10000, and dialyzed against 8 mL of phosphate buffered saline (PBS) solution (pH = 7.4) or acetate buffer solution (pH = 5.4) in a sample vial. All these samples were in triplicate and incubated in a vapor-bathing constant temperature vibrator at 37 °C. At each predetermined time interval, 1 mL of release medium was withdrawn and then 1 mL of respective fresh buffer solution was added. The released DOX was quantified using UV-vis spectrometry at 480 nm.

MTT cell viability assay and cell morphology observation

HepG2 cells were regularly cultured in 25 mL culture flask with 5 mL of DMEM (10% FBS, 1% penicillin-streptomycin) medium in a humidified incubator with 5% CO₂ at 37 °C. The next day, the medium was substituted by fresh medium consisting of PBS, LM-*m*PEG, LM-PEG-LA, free DOX, LM-*m*PEG/DOX, and LM-PEG-LA/DOX, respectively. The concentration of DOX in drug-loaded groups was set at 2 µg/mL, and the concentrations of nanocarriers were the same as those drug-loaded ones. After 24 h incubation, MTT solution (10 µL, 10 mg/mL) was added to each well. After incubation at 37 °C for 4 h, 100 µL DMSO was added to dissolve the purple MTT formazan crystal. Then, the plates were read at 570 nm using a Microplate Reader (MK3, Thermo). Mean and standard deviation for the triplicate wells for each sample were reported. In parallel, before MTT assay, the morphology of cells after treatment for 24 h was observed using a Leica DM IL LED inverted phase contrast microscope with a magnification of 200× for each sample.

To better evaluate their therapeutic efficacy, HepG2 cells were treated with LM-PEG-LA/DOX, LM-*m*PEG/DOX and free DOX at the final drug concentration of 0.4, 0.8, 1.2, 1.6, and 2.0 µg/mL for 24 h. The cell viability was measured by standard MTT assays as described previously.

Confocal microscopy

Confocal microscopy (Carl Zeiss LSM 700, Jena, Germany) was used to observe the cellular uptake of the LM-PEG-LA/DOX and LM-*m*PEG/DOX according to our previous report.³¹ Briefly, cover slips with a diameter of 14 mm were sequentially treated with 5% HCl, 30% HNO₃, and 75% alcohol and then fixed in a 24-well tissue culture plate. In this study, MCF-7 cells with low level of ASGPR expression were used as negative control, and cultured in MEM (10% heat-inactivated FBS, 1% penicillin-streptomycin) medium in a humidified incubator with 5% CO₂ at 37 °C.²³ 5×10⁴ HepG2 cells or MCF-7 cells were seeded into each well with 1 mL fresh medium and cultured at 37 °C and 5% CO₂ for 12 h to allow the cells to attach onto the cover slips. Then, the

medium was discarded, and 1 mL fresh medium containing PBS (control), free DOX, LM-*m*PEG/DOX and LM-PEG-LA/DOX with the final DOX concentration of 2 µg/mL was added into each well. The cells were incubated at 37 °C and 5% CO₂ for another 4 h. After that, the cells were rinsed with PBS for 3 times, fixed with glutaraldehyde (2.5%) for 15 min at 4 °C, and counterstained with Hoechst 33342 (1 mg/mL) for 15 min at 37 °C using a standard procedure. The DOX fluorescence was excited with a 488 nm argon blue laser, and the emission was collected through a 505-525 nm barrier filter. Finally, the samples were imaged using a 63×oil-immersion objective lens.

Flow cytometry

Flow cytometry was used to detect the targeting efficacy of LM-PEG-LA/DOX and LM-*m*PEG/DOX. Approximately 2×10⁵ HepG2 cells or MCF-7 cells per well were separately seeded in 24-well plates the day before the experiments to bring the cells to confluence. Then the medium was replaced with 1 mL fresh medium containing PBS, free DOX, LM-PEG-LA/DOX or LM-*m*PEG/DOX at DOX concentration of 2 µg/mL. After 4 h incubation, the cells were rinsed with PBS for 3 times, trypsinized, centrifugated, resuspended in PBS, and analyzed using a Becton Dickinson FACS Calibur flow cytometer equipped with an argon laser (488 nm). The DOX fluorescence of 1×10⁴ cells was measured and the mean fluorescence was quantified from the gated viable cells.

Targeted cancer cell inhibition

To explore the targeted cancer cell inhibition effect, HepG2 cells were seeded into a 96-well plate with a density of 1×10⁴ per well. After cultured for 24 h to bring the cells to confluence, the medium was replaced with 200 µL fresh medium containing free DOX, LM-*m*PEG/DOX, and LM-PEG-LA/DOX at a final DOX concentration of 10 µg/mL. After 4 h, the medium was discarded and the cells were washed with PBS for 3 times. Then fresh medium without DOX was added and the cells were continuously cultured at 37 °C for another 24 h. Finally, the viability of cells was measured using MTT assay.

Statistical analysis

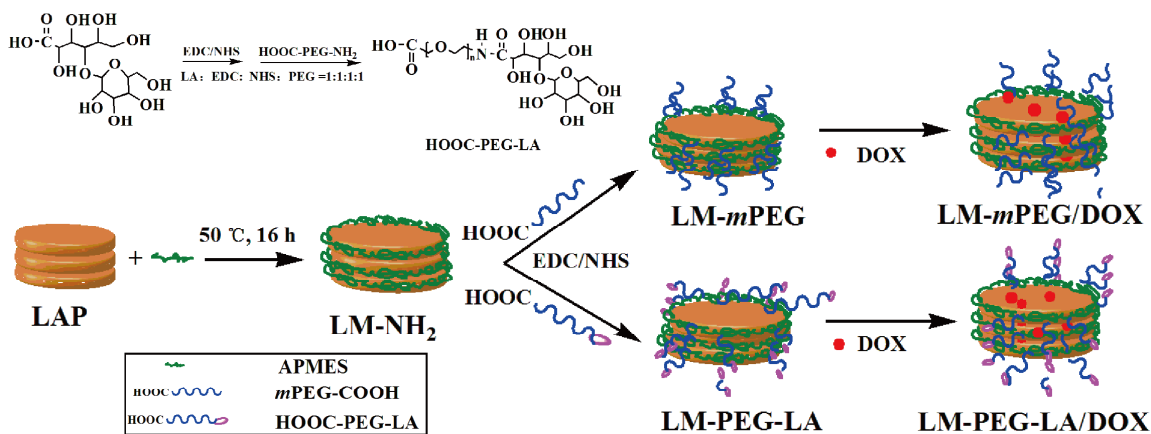
One-way ANOVA statistical analysis was performed to evaluate the experimental data. 0.05 was selected as the significance level, and the data were indicated with (*) for $p < 0.05$, (**) for $p < 0.01$, and (***) for $p < 0.001$, respectively.

Results and discussion

Synthesis and characterization of LM-PEG-LA

LAP is a layered inorganic nanomaterial with hydroxyl groups located in the interlayer space and at the edge of individual particles. It has been reported that silane coupling agents can be used to introduce new functional groups on the surface of LAP.³³ But trifunctional silane molecules may self-condense and link the clay sheets together, which may reduce the loading capacity and compromise its stability. In contrast, monofunctional silane molecules may only react at the edges of the crystalline sheets.³⁵ Therefore, in this study, monofunctional APMS was chosen to modify amine groups on the surface of LAP nanodisks at first. Then, targeting agent LA-PEG-COOH was conjugated on LM-

NH₂ via EDC chemistry in order to endow the nanodisks specific



Scheme 1 Scheme of the synthesis of LM-*m*PEG/DOX and LM-PEG-LA/DOX.

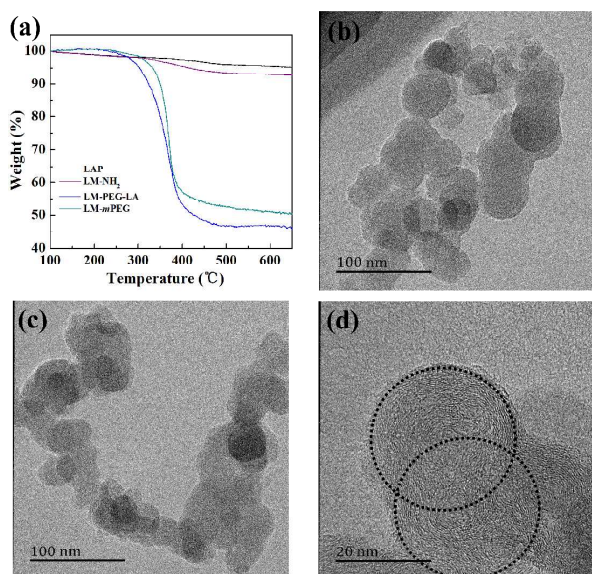


Fig. 1 (a) TGA curves of LAP, LM-NH₂, LM-*m*PEG, and LM-PEG-LA; TEM micrographs of LAP (b), and LM-PEG-LA (c, d).

delivery to hepatocarcinoma cells. It is postulated that the PEG spacer could increase the flexibility of LA and improve the colloidal stability as well.¹⁵ Finally, drug loaded LM-PEG-LA/DOX were obtained by the encapsulating of anticancer drug DOX, as shown in Scheme 1.

To demonstrate the successful surface modification of LAP, TGA analysis was carried out to measure the weight loss of LAP, LM-NH₂, LM-*m*PEG, and LM-PEG-LA (Fig. 1a). Compared with the pristine LAP, LM-NH₂ exhibited approximately 2.33% weight loss from 200 °C to 600 °C corresponding to the thermal decomposition of the organic molecules.³⁶ This result proved that silane coupling agents had been conjugated onto the surface of LAP. In the same temperature range, LM-*m*PEG and LM-PEG-LA displayed about 48.52% and 52.46% weight loss respectively, demonstrating the successful modification of *m*PEG and PEG-LA. And the higher weight loss of LM-PEG-LA than LM-*m*PEG may results from the additional LA modification on nanodisks (about 3.94 wt%). Furthermore, the successful modification can be proved directly through the TEM micrographs of LAP (Fig. 1b)

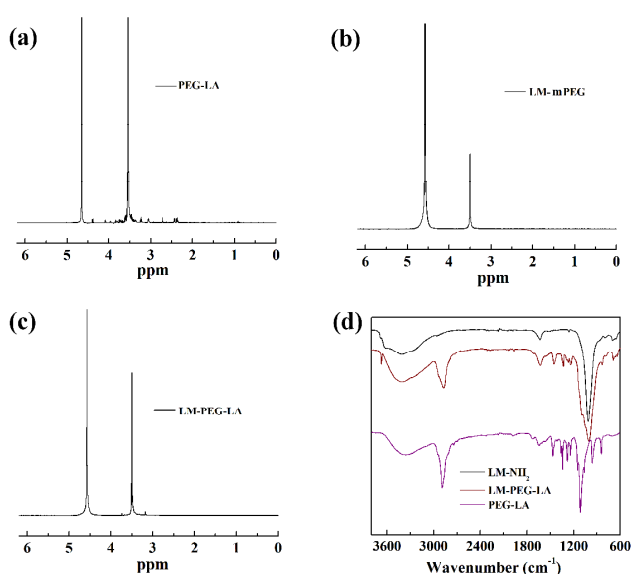


Fig. 2 ¹H NMR spectra of PEG-LA(a), LM-*m*PEG(b), and LM-PEG-LA(c); FTIR spectra of LM-NH₂, LM-PEG-LA, and PEG-LA (d).

and LM-PEG-LA (Fig 1c,1d). LAP nanodisks showed a round shape with a clear boundary at diameter of about 30 nm. In contrast, grey shadows appeared on the outlayer of LM-PEG-LA nanodisks, indicating the successful coverage of polymer (PEG-LA) on the surface of LAP nanodisks.

The chemical structure of synthesized PEG-LA, LM-PEG-LA and LM-*m*PEG were characterized by ¹H NMR spectroscopy (Fig. 2). In the spectrum of PEG-LA, the distinct peak at 3.59 ppm was assigned to the -CH₂- protons of PEG, and the proton peaks at 3.73 to 4.14 ppm were associated with LA moieties, verifying the successful synthesis of PEG-LA.^{37, 38} And the average number of LA coupled to each PEG was estimated to be 0.72 based on NMR integration. After surface modification, a prominent peak at 3.64 ppm related to PEG appeared in the spectra of LM-*m*PEG and LM-PEG-LA, indicating that PEG chain was linked on nanodisks. The spectrum of LM-PEG-LA also displayed a peak at 3.83 ppm associated with LA, demonstrating that targeting agent LA was conjugated on LAP with a PEG spacer. FTIR

spectroscopy was also performed to confirm the surface modification of LAP (Fig.

Table 1. Zeta Potential and Hydrodynamic Diameter of LAP, LM-NH₂, LM-*m*PEG, LM-PEG-LA, LM-*m*PEG/DOX, and LM-PEG-LA/DOX.

Sample	Zeta Potential (mV)	Hydrodynamic Diameter (nm)
LAP	-39.6±0.7	86.5±5.1
LM-NH ₂	-12.0±2.0	184.0±1.9
LM- <i>m</i> PEG	-14.1±1.2	354.7±13.1
LM-PEG-LA	-13.9±1.4	335.0±12.7
LM- <i>m</i> PEG/DOX	-11.3±1.1	384.0±14.4
LM-PEG-LA/DOX	-10.8±0.7	379.0±16.1

2d for LM-PEG-LA and Fig. 2S for LM-*m*PEG). A band at 1260 cm⁻¹ appeared in the spectrum of LM-NH₂ can be assigned to the irregular stretching vibration of Si-O bond, suggesting the successful silanization reaction.³⁹ In the spectrum of LM-PEG-LA, the absorption bands around 2884, 1466, 1341, 1242, 1148 and 1105 cm⁻¹ were assigned to the CH₂ stretching and the C-O-C vibration of the ether methylene units in PEG, indicating that PEG-LA was conjugated on LAP nanodisks.^{40,41} Therefore, FTIR results were in good agreement with ¹H NMR results, confirming the successful synthesis of LM-*m*PEG and LM-PEG-LA.

Since the size and surface charge may play a crucial role in determining the fate of a drug delivery system in body, it is important for the DDS to have suitable size and good colloidal stability. Table 1 displays the hydrodynamic diameters and zeta potentials of LAP, LM-NH₂, LM-*m*PEG, and LM-PEG-LA measured by DLS. After the modification by silane coupling agents, the zeta potential of nanodisks decreased dramatically from -39.6±0.7 mV of pristine LAP to -12.0±2.0 mV of LM-NH₂. It is interesting to note that the silanization step is unable to reverse the surface potential of LAP due to the inherent large negative potential of the LAP. Meantime, the hydrodynamic diameter of LM-NH₂ expanded during the silanization step (184.0±1.9 nm). The increased size suggests that some of nanodisks aggregate slightly during the modification, and the formed LM-NH₂ has the similar colloidal stability as pristine LAP in aqueous solution. Further modification of *m*PEG or PEG-LA on nanodisks has neglectable effect on the surface potential of nanodisks, but induces a significant increase in hydrodynamic diameter as 354.7±13.1 nm of LM-*m*PEG and 335.0±12.7 nm of LM-PEG-LA. This may be attributed to the formation of some aggregates by the interaction of PEG polymer chains modified on nanodisks.⁴² And the highly solvated hydrophilic PEG chain may provide additional stability for both LM-*m*PEG and LM-PEG-LA (Table S1), which will be favorable for drug loading and delivery in body.

DOX loading and release

In our previous study, we showed that DOX molecules can be encapsulated in the interlayer space of pristine LAP with a high loading efficiency.³¹ In this study, a similar process was used to encapsulate DOX in the surface-modified nanodisks. UV-Vis spectroscopy was applied to verify the encapsulation as shown in Fig. 3a. There was no significant absorption in the spectra of pure LM-*m*PEG and LM-PEG-LA, while after loading DOX, both LM-*m*PEG/DOX and LM-PEG-LA/DOX exhibited an enhanced

absorption at 480 nm, which is a characteristic strong absorption peak of DOX. This clearly demonstrated that DOX had been incorporated in both LM-*m*PEG and LM-PEG-LA. And the drug

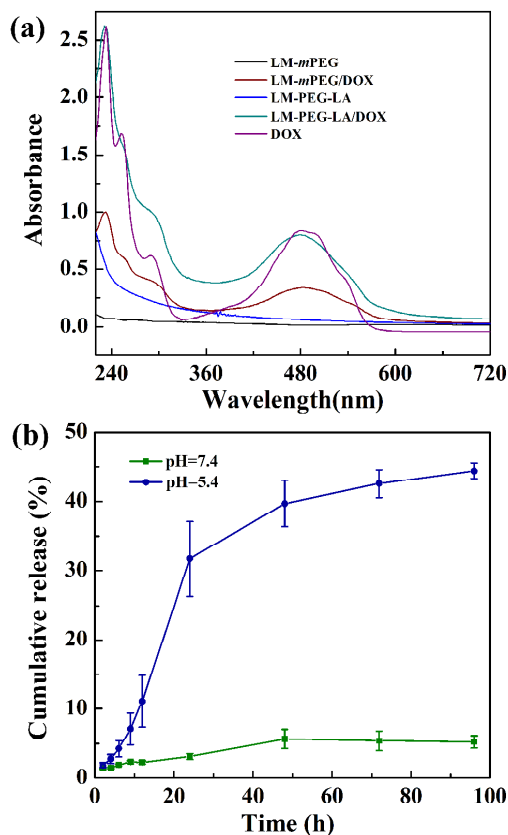


Fig. 3 (a) UV-vis spectra of DOX, LM-*m*PEG, LM-PEG-LA, LM-*m*PEG/DOX, and LM-PEG-LA/DOX; (b) In vitro release of DOX from LM-PEG-LA/DOX at 37 °C under different pH conditions.

loading efficiency and loading content of DOX in LM-PEG-LA (in LM-*m*PEG) were 91.5% (93.4%) and 30.5% (31.1%), which are similar to those of unmodified LAP. This indicated that the surface modification only happened on the edges of LAP, and would not significantly influence its interlayer structure for drug loading. Meantime, different from LAP delivery system reported in previous study,³¹ LM-*m*PEG/DOX and LM-PEG-LA/DOX showed similar zeta potential and hydrodynamic size after the encapsulation of DOX due to the additional stability provided by the PEG chains on surface (Table 1). Therefore, both LM-*m*PEG and LM-PEG-LA have a quite uniform size distribution and sufficient stability even after drug loading, which is essential for their further biomedical applications.

The release properties of DOX from LM-PEG-LA/DOX under acidic (pH = 5.4) and physiological (pH = 7.4) conditions were investigated (Fig. 3b). It can be seen that the release of DOX from LM-PEG-LA/DOX nanodisks followed a sustained manner under both pH conditions. About 45.1% DOX was released at pH 5.4 after 5 days, while only 5.2% of DOX was released at pH 7.4 at the same time point. This is likely attributed to the different solubility of DOX under different pH conditions. At an acidic condition, the salt form of DOX·HCl can be easily released from the interlayer space of LM-PEG-LA due to its good solubility. In contrast, under physiological condition, DOX is deprotonated to

form a hydrophobic neutral molecule, which may hinder the release. Therefore, DOX was released from LM-PEG-LA/DOX nanodisks with a slower rate at physiological pH than under acidic condition. This pH dependent release behavior is indeed

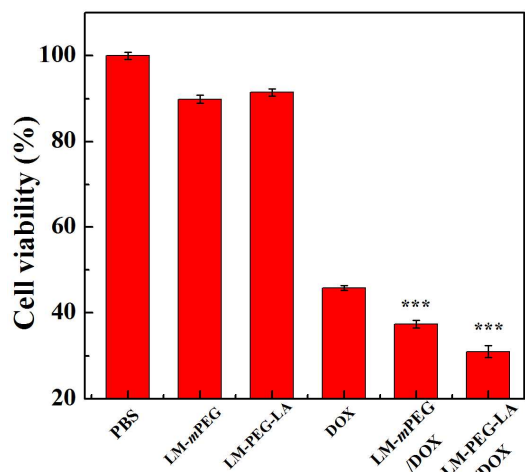


Fig. 4 In vitro MTT viability assay of HepG2 cells treated with PBS, LM-*m*PEG, LM-PEG-LA, DOX, LM-*m*PEG/DOX, and LM-PEG-LA/DOX for 24 h. The concentration of DOX in drug-loaded groups was set at 2 $\mu\text{g/mL}$. The data are expressed as mean \pm S.D. ($n=3$).

desirable for anticancer drug delivery system. The slower release at neutral pH can decrease the amount of drug released during body circulation and weaken the side effect to normal tissues, and once the drug loaded nanodisks are uptaken by cancer cells where the pH is lower, a faster release of DOX can be expected leading to better attack to tumor cells.

Antitumor efficacy of LM-PEG-LA/DOX

The antitumor efficacies of LM-*m*PEG/DOX and LM-PEG-LA/DOX were evaluated by a standard MTT colorimetric assay, and HepG2 cells with high-level ASGPR expression were used as a model cell line. Fig. 4 shows the viability of HepG2 cells after treatment with LM-*m*PEG, LM-PEG-LA, free DOX, LM-*m*PEG/DOX and LM-PEG-LA/DOX for 24 h. It appeared that over 90% of HepG2 cells were alive after being treated with LM-*m*PEG or LM-PEG-LA, indicating the good biocompatibility of synthesized carriers (more data in Fig. S2). In contrast, free DOX and drug loaded nanodisks caused a significant decrease in cell viability when compared with the untreated control ($p < 0.001$ for each). This suggested that the therapeutic activities of LM-*m*PEG/DOX and LM-PEG-LA/DOX are solely related to the loaded drug DOX. In addition, the morphology of HepG2 cells after treatment was observed in order to further confirm the biocompatibility of the synthesized carriers and the therapeutic activity of the drug-loaded complexes (Fig. S3). The HepG2 cells treated with LM-*m*PEG and LM-PEG-LA were attached on the plate and maintained their normal morphology, similar to the control group. After treatment with LM-*m*PEG/DOX and LM-PEG-LA/DOX, HepG2 cells became detached from the plate and existed in round shape, meaning that cells have undergone apoptosis just as those treated with free DOX.

To further compare the antitumor efficacy of DDS and free drugs, the cell viabilities of HepG2 cells treated with DOX, LM-*m*PEG/DOX and LM-PEG-LA/DOX at different concentrations

were evaluated as shown in Fig. 5. It can be seen that both LM-PEG-LA/DOX and LM-*m*PEG/DOX nanodisks are able to inhibit the growth of HepG2 cells in a dose-dependent manner, similar to free DOX drug. The half-maximal inhibitory concentration (IC_{50}) of DOX (1.90 $\mu\text{g/mL}$) was found to be 1.35 times higher than that

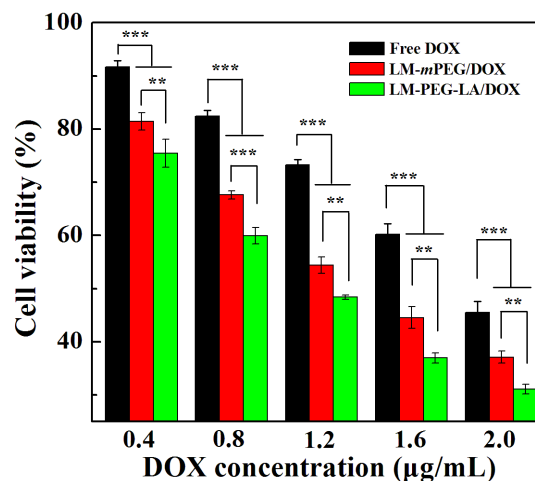


Fig. 5 In vitro MTT assay of HepG2 cells treated with DOX, LM-*m*PEG/DOX and LM-PEG-LA/DOX at different DOX concentrations for 24 h. The data are expressed as mean \pm S.D. ($n=3$).

of LM-*m*PEG/DOX (1.40 $\mu\text{g/mL}$), and 1.67 times higher than that of LM-PEG-LA/DOX (1.14 $\mu\text{g/mL}$). At the same DOX concentration, both LM-PEG-LA/DOX and LM-*m*PEG/DOX exhibited significantly higher therapeutic efficacy than DOX ($p < 0.001$), which may be attributed to the more efficient cellular uptake of DOX by the aid of nano-sized carriers. More importantly, LM-PEG-LA/DOX displayed a significantly higher inhibition of cell viability ($p < 0.01$) in comparison with LM-*m*PEG/DOX. This is likely due to the efficient cellular uptake of DOX via the receptor-mediated endocytosis between the LA modified on nanodisks and ASGPR overexpressed on liver cancer cells, which were confirmed by the FCM and CLSM data below.

Confocal microscopy and flow cytometry

To verify the intracellular uptake of LM-PEG-LA/DOX, the red fluorescence of DOX was detected via CLSM imaging (Fig. 6 for HepG2 and Fig. S4 for MCF-7 cells). Cells treated with PBS showed only Hoechst 33342-counterstained blue fluorescence in their nuclei. After 4 h of incubation with DOX, LM-*m*PEG/DOX and LM-PEG-LA/DOX, HepG2 cells displayed red fluorescence signals associated with DOX. And cells treated with LM-PEG-LA/DOX and LM-*m*PEG/DOX shows more red dots than those treated with DOX, indicating that drug-loaded nanodisks have more cellular uptake for HepG2 cells when compared with free DOX. It is worth noting that cells incubated with the drug-loaded nanodisks showed more red dots in both cytosol and cell nucleus and more aggregations around cell membrane than those treated with free DOX, suggesting the internalization of drug-loaded nanodisks, instead of the small amount of released DOX. Moreover, LM-PEG-LA/DOX nanodisks showed stronger red signals in HepG2 cell nucleus and cytosol than those treated with LM-*m*PEG/DOX, indicating the specific uptake and internalization of LM-PEG-LA/DOX nanodisks. For comparison, MCF-7 cells with low ASGPR expression displayed similar red

fluorescence signals after treated with LM-PEG-LA/DOX and LM-*m*PEG/DOX under the same experimental condition. This confirms that the modification of lactobionic acid on the surface of laponite is able to enhance the cellular uptake of LM-PEG-LA/DOX to cancer cells with high ASGPR expression.

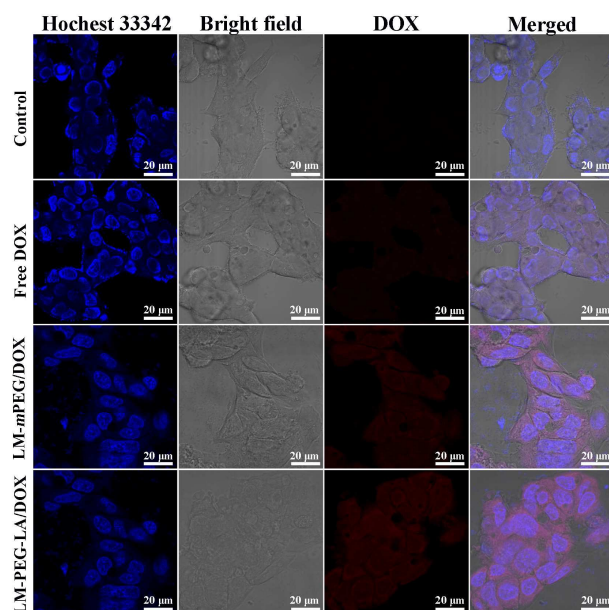


Fig. 6 CLSM images of HepG2 cells treated with PBS, free DOX, LM-*m*PEG/DOX, LM-PEG-LA/DOX with a DOX concentration of 2 µg/mL for 4 h at 37 °C.

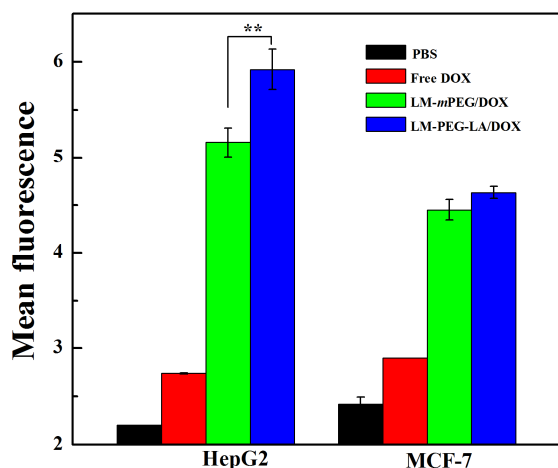


Fig. 7 Flow cytometric analysis of HepG2 and MCF-7 cells treated with free DOX, LM-*m*PEG/DOX and LM-PEG-LA/DOX at a DOX concentration of 2 µg/mL for 4 h, respectively.

FCM assay was performed to quantify the cellular uptake by incubating LM-PEG-LA/DOX or LM-*m*PEG/DOX with HepG2 cells or MCF-7 cells for 4 h (Fig. 7). Compared with the free DOX, both LM-*m*PEG/DOX and LM-PEG-LA/DOX nanodisks resulted in an obvious increase in the fluorescence signal within the cells (Fig. S5). This indicates the effective cellular uptake of LM-*m*PEG/DOX and LM-PEG-LA/DOX nanodisks, which is in agreement with the CLSM imaging data. Further quantitative FCM data revealed that HepG2 cells treated with LM-PEG-LA/DOX displayed a significantly enhanced mean fluorescence

than those with LM-*m*PEG/DOX ($p < 0.01$). In contrast, MCF-7 cells with low ASGPR expression displayed similar fluorescence intensities after treated with either LM-*m*PEG/DOX or LM-PEG-LA/DOX. This result implies that the specific cellular binding and uptake of LM-PEG-LA/DOX only occurs with cancer cells with high-level ASGPR expression. Therefore, combining the CLSM and FCM results, lactobionic acid modified LM-PEG-LA

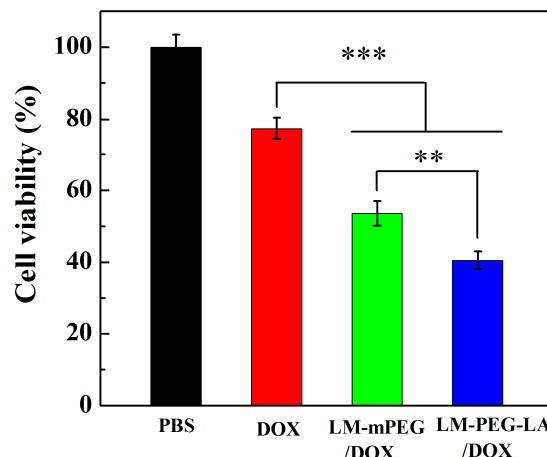


Fig. 8 MTT assay of HepG2 cells treated with free DOX, LM-*m*PEG/DOX, and LM-PEG-LA/DOX at a DOX concentration of 10 µg/mL for 4 h, followed by replacing the cell medium with DOX-free fresh medium and incubating for another 24 h.

nanodisks could specifically and efficiently deliver DOX to ASGPR-overexpressing cancer cells via receptor-mediated binding and intracellular uptake, which may result in enhanced therapeutic efficacy to target cancer cells.

Targeted therapeutic efficacy of LM-PEG-LA/DOX

To evaluate the targeted antitumor efficacy of LM-PEG-LA/DOX, HepG2 cells were separately treated with LM-*m*PEG/DOX and LM-PEG-LA/DOX for 4 h, and followed by rinsing with PBS to remove the non-bound nanodisks. Then the cells were cultured in fresh medium for 24 h before MTT assay (Fig. 8). It is clear that free DOX-treated HepG2 cells had a higher viability than those treated with LM-PEG-LA/DOX and LM-*m*PEG/DOX at the same drug concentration ($p < 0.001$), suggesting the limited cellular uptake of free DOX within 4 h. It is worth noting that the viability of HepG2 cells treated with LM-PEG-LA/DOX was much lower than those treated with LM-*m*PEG/DOX at the same DOX concentration ($p < 0.01$). Therefore, LM-PEG-LA/DOX are able to exert specific therapeutic effect to liver cells overexpressing ASGPR *via* receptor-mediated targeting (Fig. 5), which is very important for targeted drug delivery to cancer cells.

Conclusions

In summary, we successfully synthesized lactobionic acid-modified laponite nanodisks through the step-by-step surface modification of laponite with silane coupling agent and targeting agent PEG-LA. The formed nanodisks can load DOX with a high loading efficiency of 91.5% and release drug in a sustained manner with pH-responsiveness. More importantly, lactobionic acid modified laponite can specifically target HepG2 cells expressing high-level ASGPR and show a higher therapeutic

efficacy than both free DOX and untargeted ones at the same drug dosage level. Considering the facile encapsulating method, good biocompatibility and improved colloidal stability, lactobionic acid-modified laponite may serve as a targeted delivery carrier for efficient loading and specific delivery of different anticancer drugs to liver cancer cells.

Acknowledgements

This research is financially supported by the National Natural Science Foundation of China (81201189 and 21273032), the Fund of the Science and Technology Commission of Shanghai Municipality (12nm0501900), the Ph.D. Programs Foundation of Ministry of Education of China (20130075110004), and the Science and Technology Collaboration Fund between China and Hungary, Ministry of Science and Technology.

Notes and references

^a College of Chemistry, Chemical Engineering and Biotechnology, Donghua University, Shanghai 201620, People's Republic of China. E-mail: ruiguao@dhu.edu.cn, xshi@dhu.edu.cn

^b College of Materials Science and Engineering, Donghua University, Shanghai 201620, People's Republic of China.

^c Department of Biochemistry and Molecular & Cell Biology, School of Medicine, Shanghai Jiao Tong University, Shanghai 200025, People's Republic of China. E-mail: jianhuaw2007@gmail.com

† Electronic Supplementary Information (ESI) available: Additional experimental results. See DOI: 10.1039/b000000x/

‡ These authors contributed equally to this work.

1. Y. Masayuki, M. Mizue, Y. Noriko, O. Teruo, S. Yasuhisa, K. Kazunori and I. Shohei, *Journal of Controlled Release*, 1990, **11**, 269.
2. J. A. Nam, H. Mok, Y.-k. Lee and S. Y. Park, *Macromolecular Research*, 2013, **21**, 92.
3. A. Vergara-Jaque, J. Comer, L. Monsalve, F. D. González-Nilo and C. Sandoval, *J. Phys. Chem. B*, 2013, **117**, 6801.
4. P. D. Kumar, P. V. Kumar, T. P. Selvam and K. S. Rao, *Research in Biotechnology*, 2013, **4**.
5. W. Shao, A. Paul, B. Zhao, C. Lee, L. Rodes and S. Prakash, *Biomaterials*, 2013, **34**, 10109.
6. L. Wu, C. Man, H. Wang, X. Lu, Q. Ma, Y. Cai and W. Ma, *Pharmaceutical research*, 2013, **30**, 412.
7. B. D. Kevadiya and H. C. Bajaj, *Key Engineering Materials*, 2013, **571**, 111.
8. H. Maeda, H. Nakamura and J. Fang, *Advanced drug delivery reviews*, 2013, **65**, 71.
9. H. A. Kim, K. Nam and S. W. Kim, *Biomaterials*, 2014, **35**, 7543.
10. L. He, Y. Huang, H. Zhu, G. Pang, W. Zheng, Y. S. Wong and T. Chen, *Advanced Functional Materials*, 2014, **24**, 2754.
11. L. Nair, S. Jagadeeshan, A. Nair and G. V. Kumar, *PLoS one*, 2013, **8**, e70697.
12. D. Vllasaliu, L. Casertari, G. Bonacucina, M. Cespi, G. Filippo Palmieri and L. Illum, *Pharmaceutical Nanotechnology*, 2013, **1**, 184.
13. X.-y. Yang, Y.-x. Li, M. Li, L. Zhang, L.-x. Feng and N. Zhang, *Cancer letters*, 2013, **334**, 338.
14. D. Bansal, K. Yadav, V. Pandey, A. Ganeshpurkar, A. Agnihotri and N. Dubey, *Drug delivery*, 2014, **1**.
15. H. Liu, H. Wang, Y. Xu, R. Guo, S. Wen, Y. Huang, W. Liu, M. Shen, J. Zhao and G. Zhang, *ACS applied materials & interfaces*, 2014, **6**, 6944.
16. R. Villa, B. Cerroni, L. Viganò, S. Margheritelli, G. Abolafio, L. Oddo, G. Paradossi and N. Zaffaroni, *Colloids and Surfaces B: Biointerfaces*, 2013, **110**, 434.
17. P. C. Rensen, L. A. Sliedregt, M. Ferns, E. Kieviet, S. M. van Rossenberg, S. H. van Leeuwen, T. J. van Berkel and E. A. Biessen, *J. Biol. Chem.*, 2001, **276**, 37577.
18. L. W. Seymour, D. R. Ferry, D. Anderson, S. Hesslewood, P. J. Julian, R. Poyner, J. Doran, A. M. Young, S. Burtles and D. J. Kerr, *J. Clin. Oncol.*, 2002, **20**, 1668.
19. J. Wu, M. H. Nantz and M. A. Zern, *Frontiers in bioscience: a journal and virtual library*, 2002, **7**, d717.
20. A. Suo, J. Qian, Y. Yao and W. Zhang, *International journal of nanomedicine*, 2010, **5**, 1029.
21. X. Song, J. Wang, X. Luo, C. Xu, A. Zhu, R. Guo, C. Yan and P. Zhu, *Journal of Biomaterials Science, Polymer Edition*, 2014, **1**.
22. Z. Xu, L. Chen, W. Gu, Y. Gao, L. Lin, Z. Zhang, Y. Xi and Y. Li, *Biomaterials*, 2009, **30**, 226.
23. R. Guo, Y. Yao, G. Cheng, S. H. Wang, Y. Li, M. Shen, Y. Zhang, J. R. Baker, J. Wang and X. Shi, *RSC Advances*, 2012, **2**, 99.
24. C. Viseras, P. Cerezo, R. Sanchez, I. Salcedo and C. Aguzzi, *Applied Clay Science*, 2010, **48**, 291.
25. M. Ghadiri, H. Hau, W. Chrzanowski, H. Agus and R. Rohanzadeh, *RSC Advances*, 2013, **3**, 20193.
26. S. Wang, F. Zheng, Y. Huang, Y. Fang, M. Shen, M. Zhu and X. Shi, *ACS Appl. Mater. Interfaces*, 2012, **4**, 6393.
27. H. Jung, H. M. Kim, Y. B. Choy, S. J. Hwang and J. H. Choy, *Applied Clay Science*, 2008, **40**, 99.
28. H. Jung, H. M. Kim, Y. Bin Choy, S. J. Hwang and J. H. Choy, *Int. J. Pharm.*, 2008, **349**, 283.
29. M. Gonçalves, P. Figueira, D. Maciel, J. Rodrigues, X. Shi, H. Tomás and Y. Li, *Macromolecular bioscience*, 2014, **14**, 110.
30. M. Gonçalves, P. Figueira, D. Maciel, J. Rodrigues, X. Qu, C. Liu, H. Tomás and Y. Li, *Acta biomaterialia*, 2014, **10**, 300.
31. S. Wang, Y. Wu, R. Guo, Y. Huang, S. Wen, M. Shen, J. Wang and X. Shi, *Langmuir*, 2013, **29**, 5030.
32. K. Li, S. G. Wang, S. H. Wen, Y. Q. Tang, J. P. Li, X. Y. Shi and Q. H. Zhao, *ACS Appl. Mater. Interfaces*, 2014, **6**, 12328.
33. J. M. Oh, S. J. Choi, G. E. Lee, S. H. Han and J. H. Choy, *Advanced Functional Materials*, 2009, **19**, 1617.
34. P. A. Wheeler, J. Wang, J. Baker and L. J. Mathias, *Chemistry of materials*, 2005, **17**, 3012.
35. N. N. Herrera, J.-M. Letoffe, J.-L. Putaux, L. David and E. Bourgeat-Lami, *Langmuir*, 2004, **20**, 1564.
36. J. Li, Y. He, W. Sun, Y. Luo, H. Cai, Y. Pan, M. Shen, J. Xia and X. Shi, *Biomaterials*, 2014, **35**, 3666.
37. N. Bhattarai, H. R. Ramay, J. Gunn, F. A. Matsen and M. Zhang, *J. Control. Release*, 2005, **103**, 609.
38. J. Shin, P. Shum and D. H. Thompson, *J. Control. Release*, 2003, **91**, 187.
39. H. El Rassy and A. C. Pierre, *Journal of Non-Crystalline Solids*, 2005, **351**, 1603.
40. N.-P. Huang, R. Michel, J. Voros, M. Textor, R. Hofer, A. Rossi, D. L. Elbert, J. A. Hubbell and N. D. Spencer, *Langmuir*, 2000, **17**, 489.
41. T. J. Chen, T. H. Cheng, Y. C. Hung, K. T. Lin, G. C. Liu and Y. M. Wang, *Journal of Biomedical Materials Research Part A*, 2008, **87**, 165.
42. K. Shikinaka, K. Aizawa, Y. Murakami, Y. Osada, M. Tokita, J. Watanabe and K. Shigehara, *J. Colloid Interface Sci.*, 2012, **369**, 470.

Figure Captions

Scheme 1. Scheme of the synthesis of LM-*m*PEG/DOX and LM-PEG-LA/DOX.

Figure 1. (a) TGA curves of LAP, LM-NH₂, LM-*m*PEG, and LM-PEG-LA; TEM micrographs of LAP (b), and LM-PEG-LA (c, d).

Figure 2. ¹H NMR spectra of PEG-LA(a), LM-*m*PEG(b), and LM-PEG-LA(c); FTIR spectra of LM-NH₂, LM-PEG-LA, and PEG-LA (d).

Figure 3. (a) UV-vis spectra of DOX, LM-*m*PEG, LM-PEG-LA, LM-*m*PEG/DOX, and LM-PEG-LA/DOX; (b) In vitro release of DOX from LM-PEG-LA/DOX at 37 °C under different pH conditions.

Figure 4. In vitro MTT viability assay of HepG2 cells treated with PBS, LM-*m*PEG, LM-PEG-LA, DOX, LM-*m*PEG/DOX, and LM-PEG-LA/DOX for 24 h. The concentration of DOX in drug-loaded groups was set at 2 µg/mL. The data are expressed as mean ± S.D. (n = 3).

Figure 5. In vitro MTT assay of HepG2 cells treated with DOX, LM-*m*PEG/DOX and LM-PEG-LA/DOX at different DOX concentrations for 24 h. The data are expressed as mean ± S.D. (n=3).

Figure 6. CLSM images of HepG2 cells treated with PBS, free DOX, LM-*m*PEG/DOX, LM-PEG-LA/DOX with a DOX concentration of 2 µg/mL for 4 h at 37 °C.

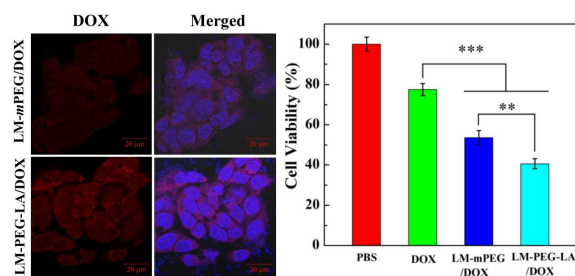
Figure 7. Flow cytometric analysis of HepG2 and MCF-7 cells treated with free DOX, LM-*m*PEG/DOX and LM-PEG-LA/DOX at a DOX concentration of 2 µg/mL for 4 h, respectively.

Figure 8. MTT assay of HepG2 cells treated with free DOX, LM-*m*PEG/DOX, and LM-PEG-LA/DOX at a DOX concentration of 10 µg/mL for 4 h, followed by replacing the cell medium with DOX-free fresh medium and incubating for another 24 h.

Table of Contents (TOC)

Targeted doxorubicin delivery to hepatocarcinoma cells by lactobionic acid-modified laponite nanodisks

Guangxiang Chen^{a,†}, Du Li^{b,‡}, Jingchao Li^a, Xueyan Cao^a, Jianhua Wang^{*c}, Xiangyang Shi^{*a,b}, Rui Guo^{*a}



Lactobionic acid-modified laponite can deliver doxorubicin specifically to hepatocarcinoma cells overexpressing asialoglycoprotein receptor and display a significantly enhanced therapeutic efficacy.